Vol. 682: 51–64, 2022
https://doi.org/10.3354/meps13923

MARINE ECOLOGY PROGRESS SERIES
Mar Ecol Prog Ser

Published January 20

Ocean acidification reduces the growth of two Southern Ocean phytoplankton

Sarah M. Andrew[1,3,*], Robert F. Strzepek[2], Oscar Branson[1,4], Michael J. Ellwood[1]

[1]Research School of Earth Sciences, Australian National University, Canberra, ACT 0200, Australia
[2]Australian Antarctic Program Partnership, Institute for Marine and Antarctic Studies, University of Tasmania, Hobart, TAS 7004, Australia
[3]*Present address:* Department of Marine Science, University of North Carolina at Chapel Hill, NC 27514, USA
[4]*Present address:* Department of Earth Sciences, University of Cambridge, CB2 1TN, UK

ABSTRACT: Model projections for the Southern Ocean indicate that light, iron (Fe) availability, temperature and carbon dioxide (CO_2) will change concurrently in the future. We investigated the physiological responses of Southern Ocean phytoplankton to multiple variables by culturing the haptophyte *Phaeocystis antarctica* and the diatom *Chaetoceros flexuosus* under various combinations of light, Fe, temperature and CO_2. Using statistical models, the influence of each environmental variable was analysed for each physiological response, ultimately predicting how 'future' conditions (high temperature and high CO_2) would influence the 2 phytoplankton species. Under future conditions, cellular chlorophyll *a* and carbon to nitrogen molar ratios were modelled to increase for both species in all light and Fe treatments, but at times were inconsistent with measured values. Measured and modelled values of the photochemical efficiency of photosystem II (F_v/F_m) declined in cultures of *P. antarctica* due to concurrent increases in temperature and CO_2, under all light and Fe treatments. The trends in F_v/F_m for *C. flexuosus* were less clear. Our model and observations suggest that when temperature and CO_2 are concurrently increased, the growth of both species remains largely unchanged. This modelling analysis reveals that high CO_2 exerts a strong negative influence on the growth of both phytoplankton, and any 'future' increase in growth can be attributed to the positive effect of warming rather than a CO_2 fertilisation effect.

KEY WORDS: Iron · Light · Temperature · Photosynthesis · Climate change

1. INTRODUCTION

The Southern Ocean plays a crucial role in regulating atmospheric carbon dioxide (CO_2) concentrations due to the austral summer algal blooms and physical overturning that account for approximately 40% of the oceanic uptake of CO_2 (Fung et al. 2000). Multiple environmental variables, such as temperature, are predicted to change concurrently by the end of the century, leading to changes in the physical and chemical properties of the ocean (Doney et al. 2009, Boyd et al. 2015). Quantifying the responses of Southern Ocean phytoplankton to the predicted changes in light availability, temperature, CO_2 and nutrient supply is necessary to refine the biogeochemical models that inform global atmospheric climate simulations (e.g. PISCES; Aumont et al. 2015).

Global temperature is predicted to increase by 2–5°C by 2100 (Stocker 2014), with an increase of 2°C predicted for the Southern Ocean based on the Representative Concentration Pathway (RCP) 8.5 scenario (Ito et al. 2015). This increase in temperature may exceed the upper bounds of the thermal tolerance for many polar species (Boyd 2019) and may, therefore, have significant implications for Southern Ocean primary production. Regionally, warming may increase surface ocean stratification, reduce vertical mixing and increase irradiance in the mixed

*Corresponding author: smandrew@email.unc.edu

layer by ~1.2–18% for the Southern Ocean (Boyd et al. 2015) despite strengthening westerly winds and decreasing irradiance predicted for the ice-free open ocean (Deppeler & Davidson 2017). Changes in light availability in the Southern Ocean are regionally dependent (Boyd et al. 2015), but it is still unclear how phytoplankton productivity will respond to predicted climate changes (Deppeler & Davidson 2017).

The modern Southern Ocean is a high-nitrate low-chlorophyll region, where productivity is limited by a lack of iron (Fe). Fe plays an essential role in many metabolic pathways within phytoplankton associated with light harvesting and CO_2 assimilation (Sunda & Huntsman 1997); thus, Southern Ocean phytoplankton species have been forced to adapt to the low Fe in this region using a variety of photophysiological and molecular strategies to both increase cellular Fe supply and storage and reduce cellular Fe demand (Moreno et al. 2018, Strzepek et al. 2019). As the majority of Fe in the Southern Ocean is supplied by upwelling (Boyd & Ellwood 2010, Tagliabue et al. 2014), vertical mixing changes may decrease the Fe supply rate from the deep ocean (Fung et al. 2000). Due to the complexity of the marine Fe cycle, there are conflicting reports on the directionality of how Fe supply will change in the Southern Ocean into the future (Leung et al. 2015). One study predicts that Fe availability will decrease by ~1% south of the Polar Front, but increase by ~11% in the northern region of the Southern Ocean (including the Subantarctic zone; Boyd et al. 2015). Furthermore, under RCP 8.5, increased CO_2 within the atmosphere will invade the ocean, lowering oceanic surface pH by about 0.3–0.4 pH units (Bopp et al. 2013), decreasing the concentration of biologically available dissolved inorganic ferric species (Fe′) and reducing the biological uptake of Fe (Shi et al. 2010, McQuaid et al. 2018).

Observations of the natural Southern Ocean phytoplankton community suggest that diatoms may have a higher tolerance to very high CO_2 than the haptophyte *Phaeocystis antarctica* (Hancock et al. 2018). As a result, *Chaetoceros* species are often observed to respond positively to ocean acidification scenarios (Tortell et al. 2008, Hoppe et al. 2013). An organism's response to ocean acidification is shaped by its ability to take up the increasingly available carbon substrate ($CO_{2\ aq}$) and balance the increasing stressful declines in seawater pH that occur alongside increasing CO_2 (Paul & Bach 2020). Phytoplankton may cope with pH stress in a variety of ways: by redirecting cellular energy expenditure through the down-regulation of carbon concentrating mechanisms (CCMs) as CO_2 increases, changing intracellular pH or increasing respiration (Shi et al. 2019). Increases in CO_2 alone up to a certain threshold may either stimulate or not change the growth of many phytoplankton species (Hancock et al. 2018), but it is clear that concurrent changes in CO_2 with other environmental variables, such as temperature, light and Fe, will alter the tolerance of a species to high CO_2–low pH (Hoppe et al. 2015, Passow & Laws 2015, Trimborn et al. 2019).

Our study measured the physiological effects of multiple stressors (light, Fe, temperature and CO_2) on 2 ecologically relevant Southern Ocean phytoplankton: the haptophyte *P. antarctica* and the diatom *Chaetoceros flexuosus*. A trace-metal clean ocean acidification system utilising a light–Fe–temperature–CO_2 matrix was used to examine the interactive effects between the variables. An important aim of this study was to contribute a greater understanding of how Southern Ocean phytoplankton may respond to climate change and explore the effects of environmental variables on cellular processes. Increased light, temperature and CO_2 are predicted to stimulate different photosynthetic mechanisms through (1) the increase of light energy available to drive Photosystem II; (2) the increase of temperature-dependent reaction rates of ribulose-1,5-bisphosphate carboxylase-oxygenase (rubisco); and (3) the down-regulation of CCMs expected due to high CO_2 (Falkowski & Raven 2013, Young et al. 2015). Therefore, we hypothesized that while the combination of high light, temperature and CO_2 would stimulate growth in Fe-replete cultures, it would also exacerbate Fe limitation, leading to reduced growth rates as organisms are unable to meet the cellular Fe requirements to support the increased photosynthetic electron transport and enzyme reaction rates at high light and temperature.

2. MATERIALS AND METHODS

2.1. Study organisms and culturing medium

The haptophyte *Phaeocystis antarctica* (Clone SX9) was isolated from water collected in the Australasian sector of the Southern Ocean (62° 08.72′ S, 174° 08.94′ E) in December 2004 (Strzepek et al. 2012). The Southern Ocean diatom *Chaetoceros flexuosus* was isolated from seawater collected in November 2001 from 57° 51.10′ S, 139° 50.70′ E (Strzepek et al. 2011).

The artificial seawater medium Aquil (Price et al. 1989) was used for culturing. The Aquil medium was

microwave-sterilized by microwaving for 3 cycles of 3 min and mixing in between heating cycles (Keller et al. 1988). Aquil was enriched with filter-sterilized (0.2 µm, Gelman Acrodisc PF) trace metals and vitamins and chelexed macronutrients (nitrate: 300 µmol l^{-1}, silicate: 100 µmol l^{-1}, phosphate: 10 µmol l^{-1}). Previously reported methods were used to select Fe-replete versus Fe-limiting conditions (Strzepek et al. 2011); experimental conditions are listed in Table 1. In Fe-replete treatments, the synthetic ligand EDTA was used to buffer Fe and other added trace metals (cobalt, copper, manganese, zinc) in solution. Fe-replete cultures were grown in Aquil medium containing 10 µmol l^{-1} EDTA and 58 nmol l^{-1} Fe, which was added as a filter-sterilized Fe–EDTA complex (1:1). Values for [Fe′] were calculated using Visual MINTEQ (version 3.0; default thermodynamic database) and corrected for light and pH using the calculations of Sunda & Huntsman (2003) as described in Strzepek et al. (2011).

In order to induce steady-state Fe limitation, the siderophore desferrioxamine B mesylate (DFB) was added to culture media because of its ability to strongly complex Fe. Fe-limited media were prepared using a premixed solution containing 3.5 nmol l^{-1} $FeCl_3$ complexed with 40 or 400 nmol l^{-1} of DFB and added to Aquil medium containing 10 µmol l^{-1} of EDTA to buffer the other trace metals as described in Strzepek et al. (2011). The Fe-limiting media were designed to reduce phytoplankton growth rates by ~50% at growth saturating irradiance (Strzepek et al. 2011). Therefore, the Fe:DFB ratios (nmol:nmol) of the Aquil media differed between species: for *P. antarctica*, the Fe:DFB ratio was 3.5:400; for *C. flexuosus*, Fe:DFB was 3.5:40.

2.2. Light, temperature and pH manipulation experiments

All experimental cultures were grown in triplicate 1 l polycarbonate bottles (Nalgene) and allowed to acclimate to experimental conditions for at least 2 transfers (approximately 20 cell divisions) before starting the experiment. Initial experiments were conducted to determine the point at which biomass altered the pH of the growth medium, and cultures were maintained in exponential phase by dilution before this point to maintain stable medium pH. Experimental cultures were grown under each experimental treatment for at least 3 transfers (30 generations) before experiments were terminated. Cultures were grown under continuous light at 2 photon flux densities (20 and 200 µmol photons m^{-2} s^{-1}; Philips Alto II fluorescent tubes) and 2 temperatures: 3.0 ± 0.1°C (temperature at which species were isolated; Andrew et al. 2019) and 5.0 ± 0.1°C (predicted warming of 2°C in the Southern Ocean). Continuous light was chosen instead of a light–dark cycle to remove any sampling artefacts associated with the cyclic behaviour in the growth rates and other physiological rates that is imposed by a light–dark regime (Strzepek et al. 2011, Hoppe et al. 2015). The low irradiance used (20 µmol photons m^{-2} s^{-1}) is representative of a deep spring mixed layer, while the high irradiance (200 µmol photons m^{-2} s^{-1}) is above the average values observed in a typical summer mixed layer (Hopkinson et al. 2013). Experimental cultures of *P. antarctica* and *C. flexuosus* were also grown under 2 CO_2 levels: a low-CO_2 treatment and a high-CO_2 treatment. The first was an ambient laboratory CO_2 treatment, using a closed system and with no manipulation of the carbonate system (>400 µatm at room temperature, calculated to equal 202–211 µatm at the experimental temperature; Table 2). This treatment is directly comparable to other Southern Ocean culturing

Table 1. Environmental conditions used in this study and calculated values for free iron concentrations [Fe′]. Note that in the final 2 columns, Fe′ values for desferrioxamine B mesylate (DFB) treatments are estimates, as no information is available to calculate how Fe′ may change with pH, light or temperature when Fe is bound to DFB

Experimental treatment	Irradiance (µmol photons m^{-2} s^{-1})	Species and free iron concentrations [Fe′] (pmol l^{-1})		
		Phaeocystis antarctica and *Chaetoceros flexuosus* 58 nmol l^{-1} Fe; 10 µmol l^{-1} EDTA; high iron	*P. antarctica* Fe:DFB 4:400 (nmol:nmol); low iron	*C. flexuosus* Fe:DFB 4:40 (nmol:nmol); low iron
3°C	200	4375	0.02	0.19
	20	784	0.02	0.19
3°C + CO_2	200	1456	0.02	0.19
	20	177	0.02	0.19
5°C	200	3539	0.02	0.19
	20	700	0.02	0.19
5°C + CO_2	200	1223	0.02	0.19
	20	155	0.02	0.19

Table 2. Measured pH (total scale) and total alkalinity (TA) (both measured at room temperature) and the calculated pCO_2 (calculated at *in situ* temp) for each experimental treatment over the total duration of the experiment (>3 yr). Data are presented as averages ± SD for all biological replicates; n = the combined number of biological replicates for *Phaeocystis antarctica* and *Chaetoceros flexuosus* measured at the beginning and end of each experimental treatment

Experimental treatment	Biological replicates (n)	Measured pH (total scale)	Measured TA (µmol kg^{-1})	Calculated pCO_2 (µatm)
3°C[a]	96	8.07 ± 0.09	2334 ± 72.4	202 ± 59
3°C + CO_2	144	7.46 ± 0.32	2468 ± 156	1278 ± 384
5°C[a]	96	8.13 ± 0.18	2359 ± 153	211 ± 54
5°C + CO_2	168	7.64 ± 0.16	2542 ± 122	1149 ± 273

[a]Closed system, carbonate chemistry not altered

studies (e.g. Andrew et al. 2019, Strzepek et al. 2019) and is within the lower range of *in situ* values for partial pressure of (pCO_2) (Takao et al. 2020). This low-CO_2 treatment can be considered growth-saturating for *P. antarctica* and probably close to saturating for *C. flexuosus* (Zhu et al. 2017). The elevated CO_2 treatment of ~1000 µatm was obtained using a trace-metal clean, CO_2-controlled incubator system adapted from Hoffmann et al. (2013). Mass flow controllers (Omega FMA5502A and FMA5518A) were used to create a CO_2–air mixture of the desired CO_2 concentration that was monitored daily with a CO_2 probe (K30 10 000 ppm Sensor Module; www.CO2Meter.com) to validate the calculated seawater chemistry parameters described below. Early to mid-exponential phase cultures from the corresponding low-CO_2 treatment were acclimated to high-CO_2 conditions by increasing CO_2 to 1000 µatm over 10 generations using the CO_2-controlled incubator system. After pre-acclimation, seawater was equilibrated to the target CO_2 level at the experimental temperature before being inoculated with the desired species. In addition to continuously logging pCO_2 by a CO_2 sensor, carbonate systems measurements were taken from the culture medium before the addition of cells at the beginning of the experiment and periodically throughout the experiment (Table 2).

2.3. Seawater chemistry

Total alkalinity (TA) and pH (total scale) measurements were determined spectrophotometrically (Dickson et al. 2007, Nand & Ellwood 2018) using purified bromophenol blue indicator dye and purified *m*-cresol purple, respectively. UV-vis (Cary WinUV) measurements were made at 25°C. Measurements for TA and pH were replicated 3 times to determine precision. A filtered seawater medium was used to blank the instrument at each wavelength before readings were recorded. Instrument drift was accounted for by subtracting a reading at a reference wavelength (730 nm) from the measurements. Samples were kept in a sealed flask to ensure no degassing (Riebesell et al. 2011) while being brought up to room temperature (3°C + CO_2, 5°C + CO_2; 5°C treatments measured at 15°C, 3°C treatments measured at 25°C). These measurements were then adjusted to calculate pCO_2 at either 3 or 5°C using CO_2SYS (Pierrot et al. 2006; Table 2). In this study, we report the range of carbonate system measurements taken from the entire duration of the experiment, thus considering variation in the basal medium whilst also capturing the increase in atmospheric pCO_2 over time, similar to Cavalcanti et al. (2018) and Clark et al. (2020).

2.4. Growth rate measurements

Triplicate cultures were maintained in exponential growth by a 1:100 dilution by transfer into fresh medium as required. Growth data were collected for each culture acclimated to experimental temperature, irradiance, Fe or CO_2 treatments for a minimum of 30 generations (3 continuous transfers, n ≥ 9 for each experimental treatment). *In vivo* chlorophyll *a* (chl *a*) fluorescence of acclimated cultures was measured using a Turner Designs model 10-AU fluorometer. Specific growth rates (µ, d^{-1}) were determined from least-squares regressions of the natural logarithmic increase in *in vivo* fluorescence versus time during the exponential phase of growth (Brand et al. 1981).

2.5. Cellular carbon, nitrogen and chl *a* concentrations and fast repetition rate fluorometry

Measurements of cell density and volumes, *in vitro* chl *a*, carbon and nitrogen content (C:N) and fast repetition rate fluorometry (LIFT FRR fluorometer; Soliense) were made on mid-exponential phase cultures as previously described (Andrew et al. 2019). Triplicate samples (1 ml) for mean cell volume

and culture cell density for *P. antarctica* were determined by Coulter Counter® (Model MS4), and cell diameters were calculated assuming a spherical geometry. To determine the percentage of cells occurring within colonies, 400 µl of glutaraldehyde was added to the analysed sample and remeasured, and the number of cells in colonies was calculated by difference (Luxem et al. 2017). Cell counting and sizing of the diatoms was done by light microscopy using a 1 ml Sedwick Rafter counting chamber. Diatoms were preserved in 2% glutaraldehyde and counted within 7 d of harvest. To estimate the cell volume and surface area of *C. flexuosus*, at least 50 individual cells for each biological replicate from each treatment were measured to obtain average frustule dimensions. Cell volume was estimated using a cylindrical geometry for *C. flexuosus* (Hillebrand et al. 1999).

2.6. Statistical analyses

The experimental design of this work required 4 environmental variables to be manipulated: temperature, CO_2, light and Fe availability. These are our independent variables. Each independent variable has 2 states, yielding a total of $2^4 = 16$ experimental conditions. In each experimental condition, 6 dependent variables were measured: mean cell volume, chl *a*, C:N ratio, the photochemical efficiency and functional absorption cross-section of photosystem II (F_v/F_m and σ_{PSII}, respectively) and µ. Because of the nature of the experimental design and time required to undertake each treatment, we were not able to generate the number of replicates needed to apply common frequentist statistical approaches (e.g. ANOVA). Instead, we adopted a 'model selection' approach similar to that of Boyd et al. (2016) to identify patterns in the data. Model evaluation was conducted in Python using the 'brutefit' module (https://github.com/oscarbranson/brutefit, doi:10.5281/zenodo.3364898), which compares candidate models using their Bayes factors relative to a null model using the method of Liang et al. (2008). Brutefit also makes extensive use of the 'numpy' (Harris et al. 2020), 'pandas' (McKinney 2011, doi:10.5281/zenodo.3509134) and 'scikit-learn' (Pedregosa et al. 2011) libraries. The python code is provided in Supplement 1 at www.int-res.com/articles/suppl/m682p051_supp/.

Boyd et al. (2016) explored the relative importance of independent variables in their data by comparing 5 arbitrary models, which included or excluded independent variables. The relative skill of these models to predict patterns in their data was used to measure the importance of each independent variable in their analysis. Our approach expands on this process to compare the skill of all possible linear models to explain the data. With 4 independent variables, this yielded 112 candidate models which encompassed all permutations of linear and interactive terms (Figs. S1 & S2 in Supplement 2). Before analysis, data were normalised to a mean of zero and a standard deviation of one. This approach allows interpretation of the relative importance of each parameter in the data across their range in our experiments, which is calculated by combining the effect size of each covariate in every candidate model weighted by their Bayes factors. This calculation produces a probability density distribution that describes the effect size of each covariate in all candidate models, where better fitting models contribute more strongly to the distribution. This approach evaluates relationships present in the data while making no assumptions about the form of the underlying model or the normality of model residuals.

3. RESULTS

3.1. Individual and interactive effects of light, Fe, temperature and CO_2

Specific growth rates of *Chaetoceros flexuosus* were highest in cultures grown in the 5°C high-light, high-Fe (HL Fe+), low-CO_2 treatment (0.57 ± 0.11 d^{-1}) while the lowest growth rates of *C. flexuosus* were observed in the 5°C low-light, low-Fe (LL Fe–), low-CO_2 treatment (0.15 ± 0.05 d^{-1}). Growth rates of *Phaeocystis antarctica* ranged from 0.64 ± 0.05 in the 5°C HL Fe+, low-CO_2 treatment to 0.14 ± 0.06 in the 5°C LL Fe–, high-CO_2 treatment (Fig. 1, Table S1 in Supplement 3).

The highest F_v/F_m was observed in cultures grown under HL Fe+ and low-CO_2 treatments for both species (*C. flexuosus*: 0.55 ± 0.02 at 5°C; *P. antarctica*: 0.58 ± 0.02 at 3°C; Fig. 2). The lowest F_v/F_m values (0.20 ± 0.04) were observed in cultures of *C. flexuosus* grown at 3°C HL Fe– at high CO_2, while the lowest F_v/F_m in cultures of *P. antarctica* (0.18 ± 0.05) were measured at 5°C HL Fe– and high CO_2.

Maximum cellular concentrations of chl *a* normalized to cell volume (mmol l^{-1}) were observed for both *C. flexuosus* (14.2 ± 2.27 mmol l^{-1}) and *P. antarctica* (14.7 ± 1.21 mmol l^{-1}) cultures grown at 3°C under LL Fe+ and high CO_2 (Fig. 3). The lowest chl *a* concentrations (*C. flexuosus*: 1.57 ± 0.10 mmol l^{-1}; *P. antarctica*: 1.01 ± 0.10 mmol l^{-1}) were observed in cultures

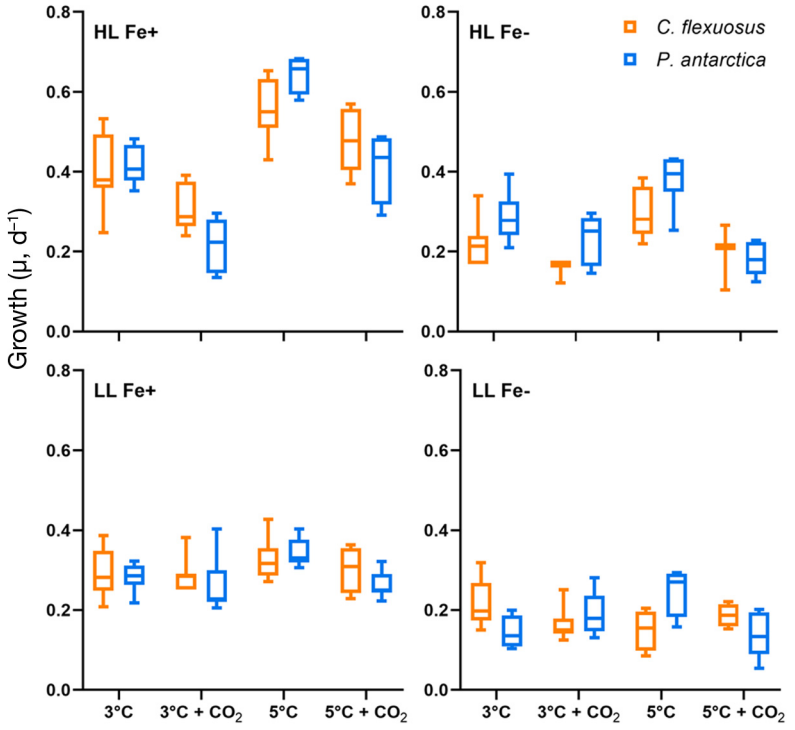

Fig. 1. Specific growth rates versus treatment for *Chaetoceros flexuosus* and *Phaeocystis antarctica* cultures grown under high (1000 µatm) and low (~200 µatm) CO_2, high (5°C) and low (3°C) temperature, high (HL) and low (LL) light and high (Fe+) and low (Fe–) Fe availability. Bar: median; box: interquartile range (IQR); whiskers: max./min. values <1.5×IQR above/below box. Experimental treatments are described in Table 1; n > 9

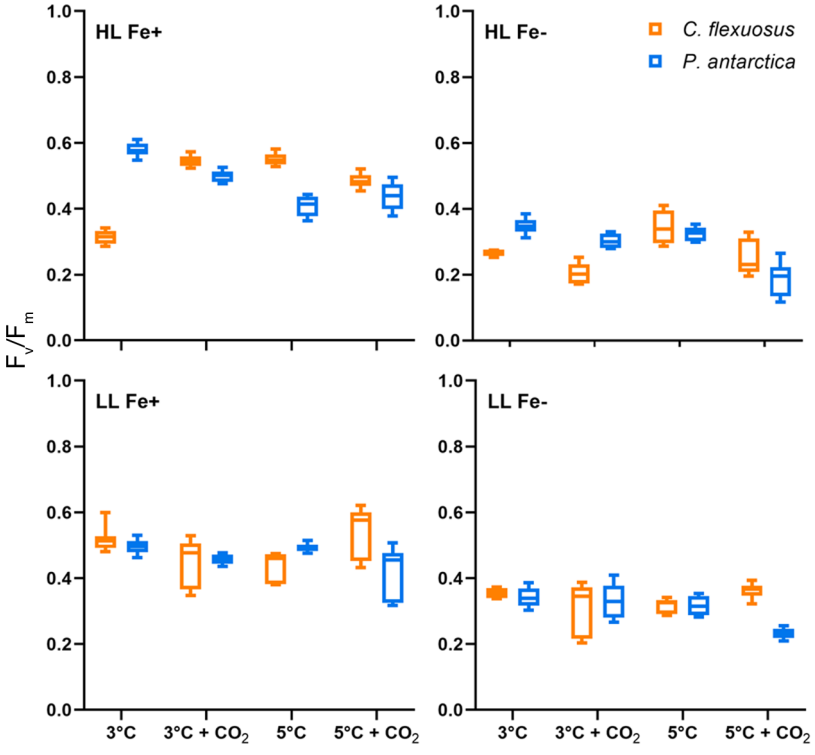

Fig. 2. As in Fig. 1, but for photochemical efficiency of PSII (F_v/F_m) versus treatment for *Chaetoceros flexuosus* and *Phaeocystis antarctica*; n = 12

grown at 3°C under HL Fe– and low CO_2.

The molar ratio of C:N differed between species in response to changing experimental variables (Fig. 4). C:N ratios ranged from 4.27 ± 0.30 mol:mol (3°C, LL Fe– and high CO_2) to 8.48 ± 0.22 mol:mol (5°C, LL Fe+ and low CO_2) for *C. flexuosus*. In cultures of *P. antarctica*, the C:N ratio was lowest in the 3°C, LL Fe– and low-CO_2 treatment (4.19 ± 0.28) and highest in the 5°C, LL Fe+ and high-CO_2 treatment (9.90 ± 0.75).

P. antarctica can form colonies as part of its life cycle, which may play a significant role in C export during blooms (DiTullio et al. 2000). Similar to prior work, at 3°C and low CO_2 few colonies were observed, with close to 100% of cells occurring as solitary cells under Fe– conditions (Table S1) and approximately 60–80% occurring as single cells under Fe+ (Becquevort et al. 2007). In contrast, for cells grown at high CO_2, approximately 34–86% of the cells occurred as single cells, with no obvious influence of light, temperature or Fe.

3.2. Comparison of growth and physiological responses in a modelled future scenario

To interpret the results from our modelling approach, we purposefully steered clear of using p-values and 'significance' terminology because the small sample sizes in our study invalidates the use of standard statistical methods (e.g. ANOVA). Rather, we appraised the relative importance of our dependent variables graphically (Figs. 5 & S3 in Supplement 2). In Fig. 5, we present the size of the effect attributable to each experimental covariate determined by our linear modelling approach, with distributions that overlap with zero (by more than 5%, or p = 0.05 cutoff) removed. For each probability distribution, the location (–1 to +1) represents the relative

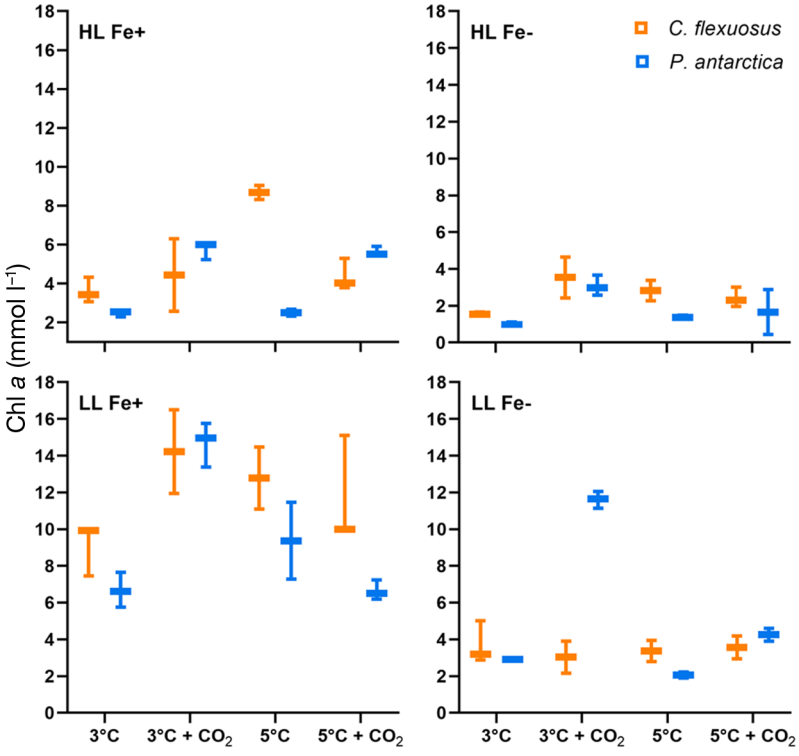

Fig. 3. As in Fig. 1, but for chlorophyll *a* normalized to cell volume versus treatment for *Chaetoceros flexuosus* and *Phaeocystis antarctica*; n = 3

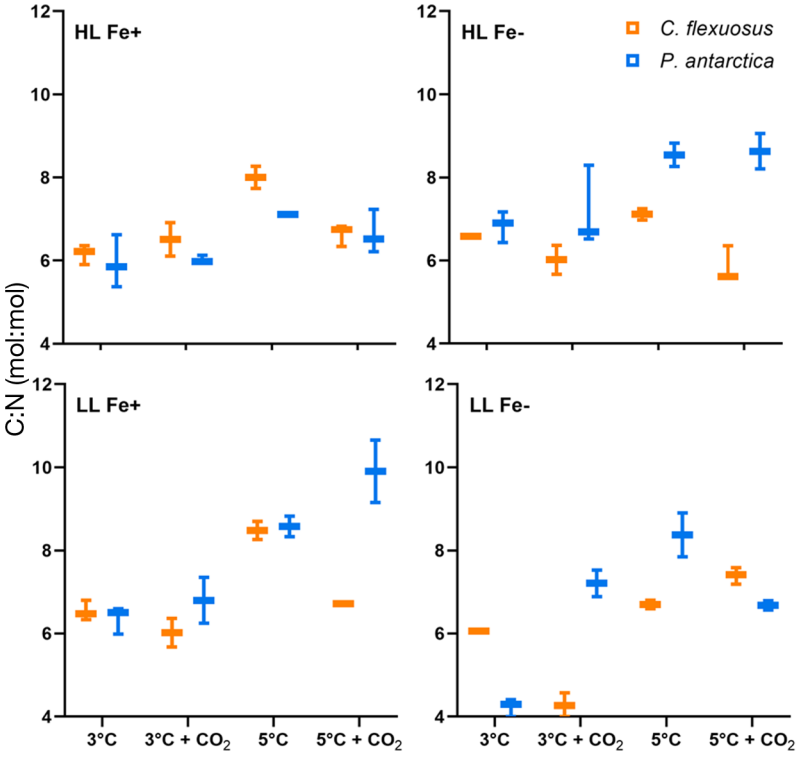

Fig. 4. As in Fig. 1, but for carbon to nitrogen molar ratio (C:N) versus treatment for *Chaetoceros flexuosus* and *Phaeocystis antarctica*; n = 3

strength of the effect observed in our data, and the shape represents how variable the effect size was across our ensemble of 112 linear models. The contribution of models to these covariate distributions was weighted according to the 'skill' of each model using the Bayes factors. If a distribution was 'sharp', the effect size of this covariate was relatively consistent across all high-skill models; i.e. its value is relatively constant despite the inclusion or exclusion of other covariates in the model. For example, the influence of Fe on growth rate is reflected as a sharp, well-defined probability density peak for these 2 physiological parameters (Fig. 5A,G). This is consistent with the classical bar graph presentation approach, where cell growth is higher for Fe-replete cells versus Fe-limited cells (Fig. 1). For probability densities with broader distribution, the importance of this covariate in the high-skill models varies with the addition or removal of other covariates, and we can be less confident in this effect. This can be interpreted as higher Fe availability having a positive influence on growth (Fig. 5A,G) but higher CO_2 having a negative influence on growth (Fig. 5A,G). If the distribution overlaps with zero, this may be interpreted as having no (or little) effect on the dependent variable — or being 'non-significant' in frequentist terminology (Fig. S3, p = 1).

To present the results of the study in a meaningful way and to move away from the classical bar graph presentation of the data, we divided the results into 2 groups: ambient, low-CO_2 culturing conditions and a future high-CO_2 ocean scenario (Fig. 6). We defined ambient, low-CO_2 culturing conditions with respect to temperature and CO_2 (temperature: 3°C; pCO_2: ~200 µatm); however, light and Fe were varied. For the future ocean scenario, temperature and CO_2 conditions were set to values expected near the end of the 21st century based on the RCP 8.5 pathway for CO_2 emissions (temperature: 5°C;

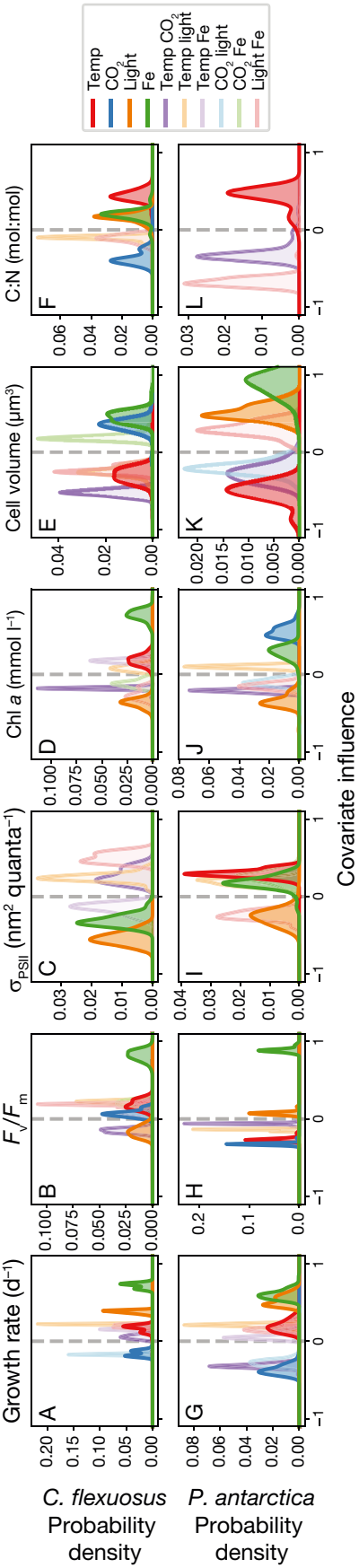

Fig. 5. Probability density plots of the size of covariate effects on measured physiological parameters for (A–F) *Chaetoceros flexuosus* and (G–L) *Phaeocystis antarctica*, determined by fitting a multivariate linear model to all data simultaneously (using a p = 0.05 cutoff). The distribution of effect sizes is calculated from the size of each parameter in all 112 models weighted by the skill of each model. Sharp peaks represent consistent effect size across all high-skill models, whereas broad distributions have less confidence across models. Probability distributions centered above zero indicate a positive influence on cell physiology

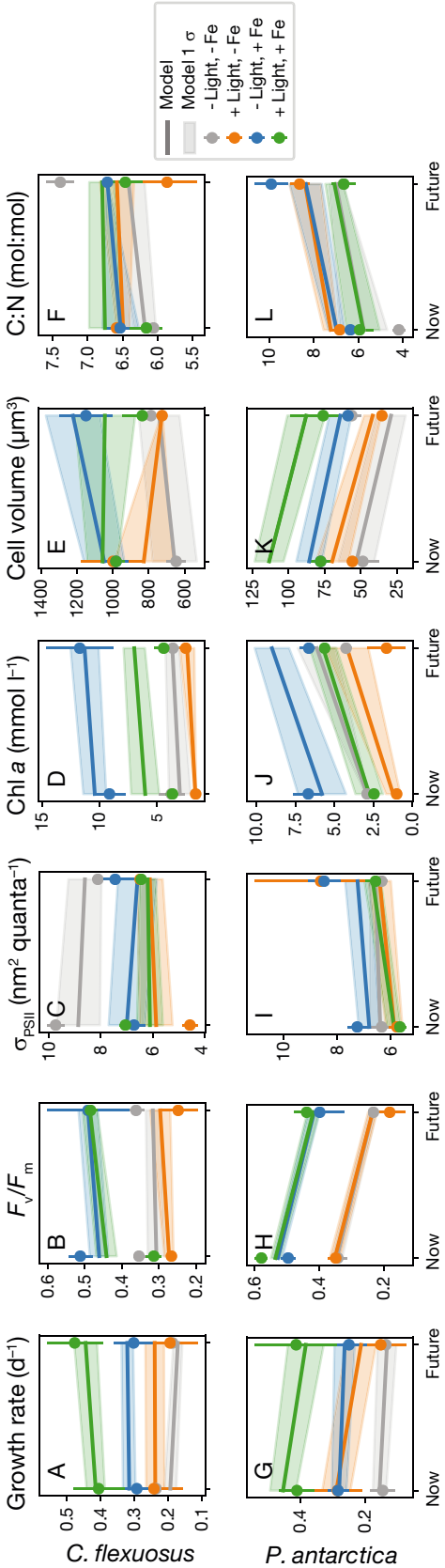

Fig. 6. Physiological and growth responses of (A–F) *Chaetoceros flexuosus* and (G–L) *Phaeocystis antarctica* for ambient, low CO_2 culturing conditions (3°C, ~200 µatm CO_2) and a future Southern Ocean scenario (5°C, ~1000 µatm CO_2) under varying iron and light conditions. Data points are average measured values ±SD for each treatment. Solid lines: individual effects identified by a multivariate model fit to all variables (Fig. 5); shaded areas: 1σ confidence interval. See Figs. S1 & S2 for further information

pCO_2: ~1000 µatm). Again, Fe and light were varied for these future scenarios. Dependent variables (growth rate, F_v/F_m, σ_{PSII}, cell volume, chl *a*, C:N ratio) are presented with the best model fit for each treatment, in addition to the measured result for each treatment (Fig. 6, Table S1).

3.2.1. Modelled responses of *C. flexuosus* to multiple stressors

Overall, when comparing growth rates in an ambient, low-CO_2 (3°C, low CO_2; referred to as 'ambient scenario' in all further instances) and future scenario (5°C, high CO_2), the highest growth rates for *C. flexuosus* were observed for the HL and Fe+ treatments for present-day (0.41 ± 0.08 d^{-1}) and future (0.47 ± 0.08 d^{-1}) scenarios (Figs. 1 & 6A). Increased Fe under HL increased growth for *C. flexuosus* under future condition scenarios, but Fe– and LL decreased growth for *C. flexuosus* under future conditions relative to ambient conditions (Fig. 6). In all cases, the measured values were similar to the predicted model. Similarly, F_v/F_m was negatively affected by HL but positively influenced by Fe+ (Fig. 5B) and modelled to increase in all future conditions (Fig. 6B).

Future values of σ_{PSII} for *C. flexuosus* were modelled to decrease under LL and increase under HL; however, the measured values sometimes fell outside of the model confidence interval (Fig. 6C) due to the conflicting influences of individual and combined stressors (Fig. 5C). Cellular chl *a* concentrations were modelled to increase under all future conditions (Fig. 6D) and were influenced mainly by Fe+ followed by warming (Fig. 5D). Changes in cell volume for *C. flexuosus* varied between ambient and future conditions with patterns depending on specific treatments; however, all modelled confidence intervals were large (Fig. 6E). For instance, under HL and Fe– conditions, cells decreased in volume, whereas the opposite occurred under LL Fe+ conditions (Fig. 6E).

3.2.2. Modelled responses of *P. antarctica* to multiple stressors

Like *C. flexuosus*, when comparing modelled growth rate responses of *P. antarctica* for an ambient scenario (3°C, low CO_2) and future scenario (5°C, high CO_2), the highest growth rates were observed for the HL and Fe+ treatments for the ambient (0.41 ± 0.08 d^{-1}) and future (0.41 ± 0.13 d^{-1}) scenarios (Figs. 1 & 6G). When Fe and light were reduced, either in combination or individually, growth for *P. antarctica* declined (Fig. 5G). Under all modelled future condition scenarios, this decline under future conditions was greater under HL (Fig. 6G). Analysis of the probability density function results suggested that elevated CO_2 was the main factor responsible for the reduction of growth rates under future condition scenarios (Fig. 5G). F_v/F_m declined under future conditions in all Fe and light treatments (Fig. 6H). Analysis of the probability density function results for *P. antarctica* indicated that high Fe exerts the strongest positive influence on F_v/F_m, with high CO_2 exerting the strongest negative influence (Fig. 5H).

Measured values of σ_{PSII} for *P. antarctica* sometimes fell outside of the model confidence intervals (Fig. 6I), influenced by conflicting interactive and combined effects of treatments (Fig. 5I). Chl *a* concentrations for *P. antarctica* were modelled to increase under all future conditions, regardless of light or Fe (Fig. 6J). Changes in cell volume for *P. antarctica* were variable with no obvious influence of treatment (Table S1), as the model fits for cell volume were generally poor (Fig. 6K), which is reflected by the broad probability densities (Fig. 5A).

The C:N ratio of both species was positively influenced by temperature (Fig. 5F,L) but negatively influenced by high CO_2 for cultures of *C. flexuosus* (Fig. 5F) or the combinations of light and Fe, and temperature and CO_2 for cultures of *P. antarctica* (Fig. 5L). For *C. flexuosus*, there were no obvious trends between observed changes in the C:N ratios and model fits for change in C:N (Fig. 6F), but C:N ratios were modelled to increase under all future scenarios for *P. antarctica* (Fig. 6L).

4. DISCUSSION

The experiments described here manipulated key environmental variables that influence phytoplankton growth rate and cellular properties, which are predicted to change in the future as global CO_2 concentrations and temperature increase. As expected, we observed that Fe and light limitation reduced growth rates and led to changes in chlorophyll synthesis and cell volume in both species due to a lack of available energy for cellular function (Moreno et al. 2018). Similar to previous observations, at low temperature (3°C), the growth of both *Phaeocystis antarctica* and *Chaetoceros flexuous* remains relatively unchanged at low and high CO_2 (Fig. 1; Trimborn et al. 2017, Zhu et al. 2017).

Differences in the life stage of *P. antarctica* (single cells vs. colonial cells) may play a role in physiological responses to environmental changes (see Beardall et al. 2009). For example, the lower surface area:volume ratio of colonial cells may be important to limit the diffusive flux of dissolved CO_2 relative to cellular demand (Table S1; Beardall et al. 2009). Although cultures of *P. antarctica* were not observed to increase in size to the same extent as *C. flexuosus*, cellular chl *a* concentration (i.e. mmol cell^{-1}, rather than mmol l^{-1}) was observed to increase ~2-fold regardless of light and Fe treatments when grown at 3°C and high CO_2. Thus, it seems that increasing CO_2 at low temperature stimulates chl *a* synthesis in both species.

4.1. Divergent responses to warming, acidification and higher irradiance

It is likely that all variables used in this study have the potential to cause a positive growth response or a stress response, which is dependent on interactions with other environmental variables (Passow & Laws 2015). The greater impact of high CO_2 on the growth rate of *P. antarctica* compared with the growth rate of *C. flexuosus* could be attributed to a critical CO_2 threshold that differs between taxa. For example, diatoms have a higher tolerance of extreme acidification than other taxa (Zhu et al. 2017, Hancock et al. 2018, Paul & Bach 2020). Our modelled probability densities can attribute phytoplankton responses to particular variables, ultimately predicting the contribution of each environmental variable to specific physiological effects (Fig. 5). This approach also allowed us to tease apart the influence of CO_2 and temperature in future climate scenarios.

A 2°C increase in temperature from 3–5°C under low-CO_2 conditions increased the growth rate of both *P. antarctica* and *C. flexuosus* under HL Fe+, consistent with the observed optimum growth temperature of 5.2°C reported for Southern Ocean phytoplankton (Coello-Camba & Agustí 2017). The increase in growth rate with temperature can be explained by an increase in enzymatic rates, such as those of rubisco, induced by higher temperature (Falkowski & Raven 2013, Boyd et al. 2016). But the stimulatory effect of temperature on growth rate was suppressed at a high CO_2 concentration (Fig. 1). The negative interactive effect of CO_2 and warming on growth rate was greater for *P. antarctica* than for *C. flexuosus* (Figs. 1 & 5). The antagonistic relationship between warming and CO_2 concentration observed in our study was not observed for *P. antarctica* grown at various CO_2 concentrations in filtered Southern Ocean seawater at 8°C compared to 2°C (Zhu et al. 2017). The high temperature (8°C) used is near the maximum temperature for growth of *P. antarctica* (10–12°C; Zhu et al. 2017, Andrew et al. 2019); thus, it is likely that high CO_2 becomes a more substantial stressor when cultures are grown at temperatures above their optimal temperature for growth (Passow & Laws 2015). Similar to our results, Xu et al. (2014) found that growth was suppressed in *P. antarctica* when temperature and CO_2 were increased concurrently (800 µatm CO_2, 6°C) with no difference between the high- and low-Fe conditions. Irradiance was also increased in concert with temperature and CO_2 in that study (Xu et al. 2014), making it unclear how important each individual stressor was in controlling the response of each species.

Our finding that increased irradiance and CO_2 exerts a strong negative effect on growth in *P. antarctica* (Fig. 5) is consistent with the observation that simultaneous increases in CO_2 and irradiance increase photoinhibition in *Phaeocystis* (Chen & Gao 2011). The down-regulation of CCMs under high CO_2 is also predicted to increase photoinhibition, as CCMs generally act as an energy sink for electrons (Raven & Johnston 1991). Increased photosensitivity under ocean acidification and high light conditions has been observed in other studies of Southern Ocean phytoplankton (Beszteri et al. 2018, Trimborn et al. 2019) and would contribute to the reduced F_v/F_m and growth observed at high light and high CO_2 in our study (Figs. 1 & 2). Warming, individually and combined with high CO_2, increased F_v/F_m in cultures of *C. flexuous* under high light, suggesting that temperature plays a key role in the alleviation of the combined light and Fe stress in *Chaetoceros* species (Fig. 2). Similarly, *P. antarctica* does not cope well with prolonged high light stress (Trimborn et al. 2017), and our modelling suggests that the concurrent increase in light and CO_2 has a negative effect on the growth of *P. antarctica* (Figs. 5 & 6). Although *P. antarctica* and Southern Ocean diatoms have been shown to share some photophysiological adaptations to low light and Fe (Strzepek et al. 2019), our data may suggest divergent responses to cope with increased temperature and CO_2.

4.2. Mechanisms for carbonation and acidification effects on phytoplankton cultures

Most phytoplankton avoid CO_2 limitation of Rubisco by employing CCMs (Raven & Geider 1988),

which act to increase the concentration of CO_2 around the active site of rubisco in the pyrenoid. It is commonly shown that CCMs are down-regulated when cells are exposed to high CO_2 (Campbell & Tyystjärvi 2012), but phytoplankton do not always translate this resultant energy saving into increased growth rates (Kranz et al. 2015, Young et al. 2015). Ultimately, it is suggested that most phytoplankton do not up-regulate C uptake when CO_2 increases (Kim et al. 2018), probably because the energy savings from down-regulating a CCM in cold water phytoplankton are minimal (Young et al. 2015). Increasing CO_2 and temperature has been reported to result in a 137% increase in cellular C quotas for *P. antarctica* (Zhu et al. 2017), but no changes in C allocation have been observed at low temperatures (Trimborn et al. 2017, Zhu et al. 2017). In our study, temperature was observed to positively influence the C:N ratio of both *P. antarctica* and *C. flexuosus*, but the individual or interactive effect of CO_2 exerted a negative influence on both species (Fig. 5C,I). We observed an increase in the cellular C quota (mol C l^{-1}) for *C. flexuosus* in the 5°C temperature treatment (Table S1), probably due to an increase in the catalytic rate of the rubisco enzyme. No increase in C quotas was observed in the high CO_2 treatment. The temperature effect on C:N ratios differed for different light or Fe treatments; thus, our model aligned poorly with measured values in this species (Fig. 6). Similar to Passow & Laws (2015), elevated CO_2 stimulated cellular C and N quotas for *P. antarctica* (Table S1), corresponding to modelled increases of C:N ratios when temperature and CO_2 increase simultaneously (Fig. 6C). We hypothesize that the excess energy resulting from the down-regulation of CCMs is allocated to fundamentally different processes for each taxa, resulting in different growth responses and elemental compositions between our study species.

It has long been thought that species-specific requirements for inorganic C and varying activity of CCMs explain physiological responses of phytoplankton exposed to increased CO_2 concentrations; thus, species-specific growth responses to increases in pCO_2 are also influenced by the accompanying decrease in pH (Liu et al. 2017, Shi et al. 2019). Recent research has also shown that diatom species employ different mechanisms to regulate pH homeostasis due to ocean acidification. For example, *Thalassiosira pseudonana* increased its respiration rate to minimize changes in intracellular pH, while *Phaeodactylum tricornutum* and *Chaetoceros muelleri* lowered their intracellular pH to maintain stable respiration rates (Shi et al. 2019). Cytosol pH is typically maintained at ~7.0–7.5, so as external pH decreases to a level near the internal pH, less energy may be required to maintain pH homeostasis (Anning et al. 1996). It is possible that *C. flexuosus* may lower intracellular pH to maintain stable respiration rates, like *C. muelleri*, thus reserving resources that could be used for cell division (Fig. 6A; Shi et al. 2019). In the Antarctic diatom *C. debilis*, high CO_2 reduced dark respiration rates (Trimborn et al. 2014) and reduced gene expression of a number of genes involved in respiration (Beszteri et al. 2018), supporting our hypothesis that *C. flexuosus* can withstand high-CO_2 treatments by lowering its intracellular pH and thus maintain stable growth rates (Fig. 6A).

Temperature affects the ability of organisms to cope with changes in external pH and to maintain intracellular pH homeostasis for cellular functionality (Smith & Raven 1979). This could partly explain the pronounced negative effects of high CO_2 at 5°C observed in the growth rate and F_v/F_m of cultures, especially under high light or low-Fe conditions (Figs. 1, 2 & 5). Declines in F_v/F_m were observed in *P. antarctica* under most high-CO_2 conditions, signalling that CO_2 interferes with the photochemical efficiency of the cell. In addition to the reduction of intracellular dissolved organic C and the resultant change in intracellular pH observed under high CO_2 (Liu et al. 2017), it may be possible that the reduced ability for cells to acquire Fe may play a role in a cell's CO_2 response. A reduction in carbonate ion concentration associated with ocean acidification reduces the ability of the ferric Fe-concentrating protein ISIP2A to acquire Fe (McQuaid et al. 2018). Regardless of mechanistic effects, high CO_2 may further exacerbate Fe stress of phytoplankton under low-Fe conditions (Shi et al. 2010, McQuaid et al. 2018).

4.3. Future controls on Southern Ocean phytoplankton productivity

Although our study focused on the effect of temperature and CO_2 on growth under a variety of light and Fe conditions, it is expected that in the future CO_2 will increase concurrently with light and temperature (Boyd et al. 2015). The aim of culture studies using multiple stressors is to improve our understanding of species responses to climate change in the future. We used a novel experimental design and multiple multimodel fits to identify how environmental variables, individually or combined, contributed

to specific physiological effects observed for 2 species of Southern Ocean phytoplankton. Our modelling analysis revealed that high CO_2 exerts a strong negative influence on the growth of both phytoplankton species, individually and in combination with light or temperature (Fig. 5). In line with our hypothesis, Fe will continue to be an important factor for stimulating growth and will continue to play an important role in regulating phytoplankton blooms and Southern Ocean biogeochemical cycles.

Many studies have reported diverse, strain-specific responses to environmental stress (Pančić et al. 2015, Luxem et al. 2017), probably as a result of high genetic diversity across isolates isolated from the same bloom (Gäbler-Schwarz et al. 2015). The important differences between species responses to individual and combined variables highlight the importance of culturing a range of species; however, our results cannot be extrapolated to the ecosystem level. For this, mesocosm-scale experiments could provide further insights. Furthermore, to improve the mechanistic understanding of how key environmental variables interact to affect physiological function, proteomic analyses would be helpful to understand how multiple biochemical pathways are impacted by complex changes to the ocean environment.

Acknowledgements. Funding for this work was provided by an Australian Government Research Training Program Stipend Scholarship (S.M.A.), the Australian Antarctic Program Partnership (AAPP ASCI000002; R.F.S.) and Australian Research Council's Discovery Program (DP170102108 and DP130100679, M.J.E.). We thank William Sunda for many helpful discussions. We also acknowledge the 3 anonymous reviewers for their valuable comments, which significantly improved the manuscript.

LITERATURE CITED

Andrew SM, Morell HT, Strzepek RF, Boyd PW, Ellwood MJ (2019) Iron availability influences the tolerance of southern ocean phytoplankton to warming and elevated irradiance. Front Mar Sci 6:681

Anning T, Nimer N, Merrett M, Brownlee C (1996) Costs and benefits of calcification in coccolithophorids. J Mar Syst 9:45–56

Aumont O, Éthé C, Tagliabue A, Bopp L, Gehlen M (2015) PISCES-v2: an ocean biogeochemical model for carbon and ecosystem studies. Geosci Model Dev 8:2465–2513

Beardall J, Allen D, Bragg J, Finkel ZV and others (2009) Allometry and stoichiometry of unicellular, colonial and multicellular phytoplankton. New Phytol 181:295–309

Becquevort S, Lancelot C, Schoemann V (2007) The role of iron in the bacterial degradation of organic matter derived from *Phaeocystis antarctica*. In: van Leeuwe MA, Stefels J, Belviso S, Lancelot C, Verity PG, Gieskes WWC (eds) *Phaeocystis*, major link in the biogeochemical cycling of climate-relevant elements. Springer, Dordrecht, p 119–135

Beszteri S, Thoms S, Benes V, Harms L, Trimborn S (2018) The response of three Southern Ocean phytoplankton species to ocean acidification and light availability: a transcriptomic study. Protist 169:958–975

Bopp L, Resplandy L, Orr JC, Doney SC and others (2013) Multiple stressors of ocean ecosystems in the 21st century: projections with CMIP5 models. Biogeosciences 10: 6225–6245

Boyd PW (2019) Physiology and iron modulate diverse responses of diatoms to a warming Southern Ocean. Nat Clim Chang 9:148–152

Boyd PW, Ellwood MJ (2010) The biogeochemical cycle of iron in the ocean. Nat Geosci 3:675–682

Boyd PW, Lennartz ST, Glover DM, Doney SC (2015) Biological ramifications of climate-change-mediated oceanic multi-stressors. Nat Clim Chang 5:71–79

Boyd P, Dillingham P, McGraw C, Armstrong E and others (2016) Physiological responses of a Southern Ocean diatom to complex future ocean conditions. Nat Clim Chang 6:207–213

Brand LE, Guillard RR, Murphy LS (1981) A method for the rapid and precise determination of acclimated phytoplankton reproduction rates. J Plankton Res 3:193–201

Campbell DA, Tyystjärvi E (2012) Parameterization of photosystem II photoinactivation and repair. Biochim Biophys Acta 1817:258–265

Cavalcanti GS, Shukla P, Morris M, Ribeiro B and others (2018) Rhodoliths holobionts in a changing ocean: host–microbes interactions mediate coralline algae resilience under ocean acidification. BMC Genomics 19:701

Chen S, Gao K (2011) Solar ultraviolet radiation and CO_2-induced ocean acidification interacts to influence the photosynthetic performance of the red tide alga *Phaeocystis globosa* (Prymnesiophyceae). Hydrobiologia 675: 105–117

Clark TD, Raby GD, Roche DG, Binning SA, Speers-Roesch B, Jutfelt F, Sundin J (2020) Ocean acidification does not impair the behaviour of coral reef fishes. Nature 577: 370–375

Coello-Camba A, Agustí S (2017) Thermal thresholds of phytoplankton growth in polar waters and their consequences for a warming polar ocean. Front Mar Sci 4:168

Deppeler SL, Davidson AT (2017) Southern Ocean phytoplankton in a changing climate. Front Mar Sci 4:40

Dickson AG, Sabine CL, Christian JR (2007) Guide to best practices for ocean CO_2 measurements. PICES Special Publication 3. North Pacific Marine Science Organization, Sidney

DiTullio GR, Grebmeier JM, Arrigo KR, Lizotte MP and others (2000) Rapid and early export of *Phaeocystis antarctica* blooms in the Ross Sea, Antarctica. Nature 404:595–598

Doney SC, Fabry VJ, Feely RA, Kleypas JA (2009) Ocean acidification: the other CO_2 problem. Annu Rev Mar Sci 1:169–192

Falkowski PG, Raven JA (2013) Aquatic photosynthesis. Princeton University Press, Princeton, NJ

Fung IY, Meyn SK, Tegen I, Doney SC, John JG, Bishop JK (2000) Iron supply and demand in the upper ocean. Global Biogeochem Cycles 14:281–295

Gäbler-Schwarz S, Medlin LK, Leese F (2015) A puzzle with many pieces: the genetic structure and diversity of *Phaeocystis antarctica* Karsten (Prymnesiophyta). Eur J Phycol 50:112–124

Hancock AM, Davidson AT, McKinlay J, McMinn A, Schulz KG, Enden RL (2018) Ocean acidification changes the structure of an Antarctic coastal protistan community. Biogeosciences 15:2393–2410

Harris CR, Millman KJ, van der Walt SJ, Gommers R and others (2020) Array programming with NumPy. Nature 585:357–362

Hillebrand H, Dürselen CD, Kirschtel D, Pollingher U, Zohary T (1999) Biovolume calculation for pelagic and benthic microalgae. J Phycol 35:403–424

Hoffmann LJ, Breitbarth E, McGraw CM, Law CS, Currie KI, Hunter KA (2013) A trace-metal clean, pH-controlled incubator system for ocean acidification incubation studies. Limnol Oceanogr Methods 11:53–61

Hopkinson BM, Seegers B, Hatta M, Measures CI, Greg Mitchell B, Barbeau KA (2013) Planktonic C:Fe ratios and carrying capacity in the southern Drake Passage. Deep Sea Res II 90:102–111

Hoppe CJ, Hassler CS, Payne CD, Tortell PD, Rost B, Trimborn S (2013) Iron limitation modulates ocean acidification effects on Southern Ocean phytoplankton communities. PLOS ONE 8:e79890

Hoppe CJ, Holtz LM, Trimborn S, Rost B (2015) Ocean acidification decreases the light-use efficiency in an Antarctic diatom under dynamic but not constant light. New Phytol 207:159–171

Ito T, Bracco A, Deutsch C, Frenzel H, Long M, Takano Y (2015) Sustained growth of the Southern Ocean carbon storage in a warming climate. Geophys Res Lett 42: 4516–4522

Keller MD, Bellows WK, Guillard RRL (1988) Microwave treatment for sterilization of phytoplankton culture media. J Exp Mar Biol Ecol 117:279–283

Kim JM, Lee K, Suh YS, Han IS (2018) Phytoplankton do not produce carbon-rich organic matter in high CO_2 oceans. Geophys Res Lett 45:4189–4197

Kranz SA, Young JN, Hopkinson BM, Goldman JA, Tortell PD, Morel FM (2015) Low temperature reduces the energetic requirement for the CO_2 concentrating mechanism in diatoms. New Phytol 205:192–201

Leung S, Cabré A, Marinov I (2015) A latitudinally banded phytoplankton response to 21st century climate change in the Southern Ocean across the CMIP5 model suite. Biogeosciences 12:5715–5734

Liang F, Paulo R, Molina G, Clyde MA, Berger JO (2008) Mixtures of *g* priors for Bayesian variable selection. J Am Stat Assoc 103:410–423

Liu N, Beardall J, Gao K (2017) Elevated CO_2 and associated seawater chemistry do not benefit a model diatom grown with increased availability of light. Aquat Microb Ecol 79:137–147

Luxem KE, Ellwood MJ, Strzepek RF (2017) Intraspecific variability in *Phaeocystis antarctica*'s response to iron and light stress. PLOS ONE 12:e0179751

McKinney W (2011) pandas: a foundational Python library for data analysis and statistics. In: Python for high performance and scientific computing 14, p 1–9

McQuaid JB, Kustka AB, Oborník M, Horák A and others (2018) Carbonate-sensitive phytotransferrin controls high-affinity iron uptake in diatoms. Nature 555:534–537

Moreno CM, Lin Y, Davies S, Monbureau E, Cassar N, Marchetti A (2018) Examination of gene repertoires and physiological responses to iron and light limitation in Southern Ocean diatoms. Polar Biol 41:679–696

Nand V, Ellwood MJ (2018) A simple colorimetric method for determining seawater alkalinity using bromophenol blue. Limnol Oceanogr Methods 16:401–410

Pančić M, Hansen PJ, Tammilehto A, Lundholm N (2015) Resilience to temperature and pH changes in a future climate change scenario in six strains of the polar diatom *Fragilariopsis cylindrus*. Biogeosciences 12:4235–4244

Passow U, Laws EA (2015) Ocean acidification as one of multiple stressors: growth response of *Thalassiosira weissflogii* (diatom) under temperature and light stress. Mar Ecol Prog Ser 541:75–90

Paul AJ, Bach LT (2020) Universal response pattern of phytoplankton growth rates to increasing CO_2. New Phytol 228:1710–1716

Pedregosa F, Varoquaux G, Gramfort A, Michel V and others (2011) scikit-learn: machine learning in Python. J Mach Learn Res 12:2825–2830

Pierrot D, Lewis E, Wallace D (2006) MS Excel program developed for CO_2 system calculations. ORNL/CDIAC-105a. Carbon Dioxide Information Analysis Center, Oak Ridge National Laboratory, Oak Ridge, TN

Price NM, Harrison GI, Hering JG, Hudson RJ, Nirel PM, Palenik B, Morel FM (1989) Preparation and chemistry of the artificial algal culture medium Aquil. Biol Oceanogr 6:443–461

Raven JA, Geider RJ (1988) Temperature and algal growth. New Phytol 110:441–461

Raven JA, Johnston AM (1991) Mechanisms of inorganic-carbon acquisition in marine phytoplankton and their implications for the use of other resources. Limnol Oceanogr 36:1701–1714

Riebesell U, Fabry VJ, Hansson L, Gattuso JP (eds) (2011) Guide to best practices for ocean acidification research and data reporting. Office for Official Publications of the European Communities, Luxembourg

Shi D, Xu Y, Hopkinson BM, Morel FM (2010) Effect of ocean acidification on iron availability to marine phytoplankton. Science 327:676–679

Shi D, Hong H, Su X, Liao L, Chang S, Lin W (2019) The physiological response of marine diatoms to ocean acidification: differential roles of seawater pCO_2 and pH. J Phycol 55:521–533

Smith FA, Raven JA (1979) Intracellular pH and its regulation. Annu Rev Plant Physiol 30:289–311

Stocker T (2014) Climate Change 2013: the physical science basis: Working Group I contribution to the Fifth Assessment Report of the Intergovernmental Panel on Climate Change. Cambridge University Press, Cambridge

Strzepek RF, Maldonado MT, Hunter KA, Frew RD, Boyd PW (2011) Adaptive strategies by Southern Ocean phytoplankton to lessen iron limitation: uptake of organically complexed iron and reduced cellular iron requirements. Limnol Oceanogr 56:1983–2002

Strzepek RF, Hunter KA, Frew RD, Harrison PJ, Boyd PW (2012) Iron-light interactions differ in Southern Ocean phytoplankton. Limnol Oceanogr 57:1182–1200

Strzepek RF, Boyd PW, Sunda WG (2019) Photosynthetic adaptation to low iron, light, and temperature in Southern Ocean phytoplankton. Proc Natl Acad Sci USA 116: 4388–4393

Sunda WG, Huntsman SA (1997) Interrelated influence of iron, light and cell size on marine phytoplankton growth. Nature 390:389–392

Sunda W, Huntsman S (2003) Effect of pH, light, and temperature on Fe–EDTA chelation and Fe hydrolysis in seawater. Mar Chem 84:35–47

Tagliabue A, Sallée JB, Bowie AR, Lévy M, Swart S, Boyd PW (2014) Surface-water iron supplies in the Southern Ocean sustained by deep winter mixing. Nat Geosci 7: 314–320

Takao S, Nakaoka SI, Hashihama F, Shimada K and others (2020) Effects of phytoplankton community composition and productivity on sea surface pCO_2 variations in the Southern Ocean. Deep Sea Res I 160:103263

Tortell PD, Payne CD, Li Y, Trimborn S and others (2008) CO_2 sensitivity of Southern Ocean phytoplankton. Geophys Res Lett 35:L04605

Trimborn S, Thoms S, Petrou K, Kranz SA, Rost B (2014) Photophysiological responses of Southern Ocean phytoplankton to changes in CO_2 concentrations: short-term versus acclimation effects. J Exp Mar Biol Ecol 451:44–54

Trimborn S, Thoms S, Brenneis T, Heiden JP, Beszteri S, Bischof K (2017) Two Southern Ocean diatoms are more sensitive to ocean acidification and changes in irradiance than the prymnesiophyte *Phaeocystis antarctica*. Physiol Plant 160:155–170

Trimborn S, Thoms S, Bischof K, Beszteri S (2019) Susceptibility of two Southern Ocean phytoplankton key species to iron limitation and high light. Front Mar Sci 6:167

Xu K, Fu FX, Hutchins DA (2014) Comparative responses of two dominant Antarctic phytoplankton taxa to interactions between ocean acidification, warming, irradiance, and iron availability. Limnol Oceanogr 59:1919–1931

Young JN, Kranz SA, Goldman JAL, Tortell PD, Morel FMM (2015) Antarctic phytoplankton down-regulate their carbon-concentrating mechanisms under high CO_2 with no change in growth rates. Mar Ecol Prog Ser 532:13–28

Zhu Z, Qu P, Gale J, Fu F, Hutchins DA (2017) Individual and interactive effects of warming and CO_2 on *Pseudonitzschia subcurvata* and *Phaeocystis antarctica*, two dominant phytoplankton from the Ross Sea, Antarctica. Biogeosciences 14:5281–5295

Editorial responsibility: Steven Lohrenz, New Bedford, Massachusetts, USA
Reviewed by: K. Petrou and 2 anonymous referees

Submitted: April 7, 2021
Accepted: October 5, 2021
Proofs received from author(s): December 6, 2021